Contrasting controls on the phosphorus concentration of suspended particulate matter under baseflow and storm event conditions in agricultural headwater streams

Richard J. Cooper [a,*], Barry G. Rawlins [b], Tobias Krueger [c], Bertrand Lézé [a], Kevin M. Hiscock [a], Nikolai Pedentchouk [a]

[a] School of Environmental Sciences, University of East Anglia, Norwich Research Park, Norwich NR4 7TJ, UK
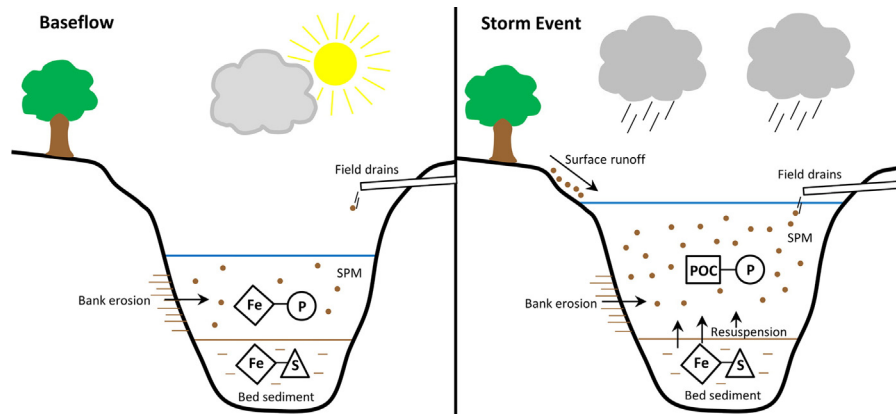[b] British Geological Survey, Keyworth, Nottingham NG12 5GG, UK
[c] IRI THESys, Humboldt University, 10099 Berlin, Germany

HIGHLIGHTS

- Controls on SPM P concentration are examined under differing stream flows.
- SPM P is dominantly associated with Fe under baseflow conditions.
- SPM P is dominantly associated with POC during storm events.
- Seasonality in the Fe–P and Al_{ox}–Al_{di} ratios of SPM are demonstrated.
- Changes in the sources of SPM are hypothesised as the causal mechanism.

GRAPHICAL ABSTRACT

Conceptual diagram of the contrasting controls on SPM phosphorus concentration in agricultural headwater streams under different hydrological conditions.

ARTICLE INFO

ABSTRACT

Whilst the processes involved in the cycling of dissolved phosphorus (P) in rivers have been extensively studied, less is known about the mechanisms controlling particulate P concentrations during small and large flows. This deficiency is addressed through an analysis of large numbers of suspended particulate matter (SPM) samples collected under baseflow ($n = 222$) and storm event ($n = 721$) conditions over a 23-month period across three agricultural headwater catchments of the River Wensum, UK. Relationships between clay mineral and metal oxyhydroxide associated elements were assessed and multiple linear regression models for the prediction of SPM P concentration under baseflow and storm event conditions were formulated. These models, which explained 71–96% of the variation in SPM P concentration, revealed a pronounced shift in P association from iron (Fe) dominated during baseflow conditions to particulate organic carbon (POC) dominated during storm events. It is hypothesised this pronounced transition in P control mechanism, which is consistent across the three study catchments, is driven by changes in SPM source area under differing hydrological conditions. In particular, changes in SPM Fe–P ratios between small and large flows suggest there are three distinct sources of SPM Fe; surface

* Corresponding author.
  E-mail address: Richard.J.Cooper@uea.ac.uk (R.J. Cooper).

Organic
Arable
Seasonality

soils, subsurface sediments and streambed iron sulphide. Further examination of weekly baseflow data also revealed seasonality in the Fe–P and aluminium oxalate–dithionate (Al_{ox}–Al_{di}) ratios of SPM, indicating temporal variability in sediment P sorption capacity. The results presented here significantly enhance our understanding of SPM P associations with soil derived organic and inorganic fractions under different flow regimes and has implications for the mitigation of P originating from different sources in agricultural catchments.

1. Introduction

Diffuse phosphorus (P) pollution is a key factor behind the development of eutrophic conditions in agricultural catchments (Withers and Jarvie, 2008; Quinton et al., 2010). As a naturally limiting nutrient of plant growth in aquatic environments, dissolved P (DP) enrichment fuels blooms of phytoplankton, periphyton and neuro-toxin secreting cyanobacteria colonies, which can dramatically lower species diversity and lead to a fundamental breakdown of ecosystem functioning (Smith et al., 1999; Hilton et al., 2006). Phosphorus is dominantly transported through rivers in particulate form, with sediment-associated P variously estimated to account for up to 90% of total P (TP) load in rural UK catchments (e.g. Walling et al., 1997; Bowes et al., 2003). However, there exists a dynamic equilibrium between the quantity of labile P associated with mineral surfaces and the concentration of DP in both soil solution (Hartikainen et al., 2010) and in stream water (Palmer-Felgate et al., 2009) which is controlled by biogeochemical processes. Consequently, understanding the importance of sediment biogeochemistry in controlling particulate P (PP) concentrations is essential if DP enrichment is to be mitigated.

Previous research has shown that DP reacts strongly with iron (Fe) and aluminium (Al) oxyhydroxide complexes in soils and stream sediments to form mineral-bearing PP phases. This occurs principally through the adsorption of phosphate ions onto solid phase mineral surfaces (non-occluded-P), followed by the subsequent absorption of phosphate ions into the mineral itself (occluded-P) (Walker and Syers, 1976; House and Denison, 2002; Evans et al., 2004). The rate at which this sorption process occurs is a function of the availability of potential P binding sites on particulate surfaces. This in turn is determined by factors such as mineral surface ionisation, presence of organic matter (OM) complexes and competition from other anions. Additionally, oxyhydroxides commonly bind to clay mineral surfaces via ligand exchange thereby forming an indirect association between P and the clay mineral component of soils and sediments (House and Warwick, 1999; Withers and Jarvie, 2008; Palmer-Felgate et al., 2009).

Although much is known about how these processes affect the instream cycling of P, less is known about how the relationships between PP and other organic and geochemical constituents change during small and large flow periods. This is important because previous research has demonstrated evidence of strong clockwise hysteresis in concentrations of both suspended particulate matter (SPM) and PP during storm events in agricultural headwater catchments (Stutter et al., 2008), thereby providing evidence of changing SPM P associations under varying flow conditions. Whilst studies by Van der Perk et al. (2007) and Rawlins (2011) developed regression models to demonstrate the importance of a range of elements (Al, Ca, Ce, Fe, K, Mn) and phases (Al/Fe oxyhydroxides, clay minerals, OM) in determining the P concentration of streambed sediments under baseflow conditions, neither study considered how these associations changed under differing flows. In fact, to our knowledge, no previous study has examined the geochemical associations between SPM and its P bearing phases under different hydrological conditions in agricultural headwater catchments. This represents a significant deficiency because source apportionment studies have demonstrated that there can be a significant change in the sources of SPM under differing flows, with subsurface inputs linked to baseflow sediment supply and increased surface source contributions associated with precipitation events (Cooper et al., 2015). Therefore, if

the sources of SPM change under different flow regimes, one can hypothesise that the organic and geochemical relationships between SPM and its P component may be similarly affected.

Therefore, the main objectives of this study were:

(i) to compare and contrast SPM organo-mineral relationships under baseflow and storm event conditions;
(ii) to develop statistical models to identify the importance of various organic and inorganic parameters in determining SPM P concentration under differing flow regimes;
(iii) to explore evidence of seasonality in SPM P concentration, Fe–P ratios and Al/Fe oxalate–dithionate ratios, and to consider what these temporal trends reveal about variability in the sources of SPM P.

This study was conducted over a 23-month period in a tributary of the lowland River Wensum, UK, and formed part of a wider investigation into the sources of fine grained SPM in this agricultural catchment.

2. Methods

2.1. Study location

This study focused on the 20 km² Blackwater sub-catchment of the River Wensum, Norfolk, UK (Fig. 1). This intensive arable headwater catchment is monitored as part of the River Wensum Demonstration Test Catchment (DTC) project which aims to evaluate the extent to which on-farm mitigation measures can cost-effectively reduce diffuse agricultural pollution whilst maintaining food production capacity (Outram et al., 2014). The Blackwater sub-catchment is divided into six 'mini-catchments' A to F for observational purposes. Each mini-catchment has a bankside kiosk at the outlet monitoring a variety of water quality parameters (e.g. pH, turbidity, temperature, ammonium, chlorophyll, dissolved oxygen, stage) at 30-min resolution. Each kiosk also encompasses an automatic water sampler (Teledyne ISCO, Lincoln, NE) containing 24, 1 L polypropylene bottles which were activated during heavy precipitation events to sample stream water.

Here, we focused solely upon mini-catchments A (5.4 km²), B (1.3 km²) and E (7.12 km²), where mini-catchments A and B are nested within mini-catchment E. Situated 30–60 m above sea level with gentle slopes (<0.5°), intensive arable land constitutes 89% of these three headwater catchments, with 8% grassland, 2% mixed woodland and 1% rural settlements. The bedrock is Cretaceous white chalk at a depth of ~20 m. Overlaying this are superficial deposits of Mid-Pleistocene diamicton glacial tills, principally chalky, flint-rich boulder clays of the Sheringham Cliffs (0.2–0.5 m depth) and Lowestoft Formations (0.5–20 m depth), interspersed with layers of glaciofluvial and glaciolacustrine sands and gravels. Superimposed on this are deposits of Late Pleistocene silty loess (cover loam) and Holocene-age alluvium and river terrace material. The principal surface soil types are clay loam to sandy clay loam to a depth of >0.2 m (Hiscock et al., 1996; Lewis, 2011). A weather station at the outlet to mini-catchment A recorded average precipitation totals of 808 mm y^{-1} and mean average annual temperatures of 9.2 °C during the April 2012–March 2014 monitoring period.
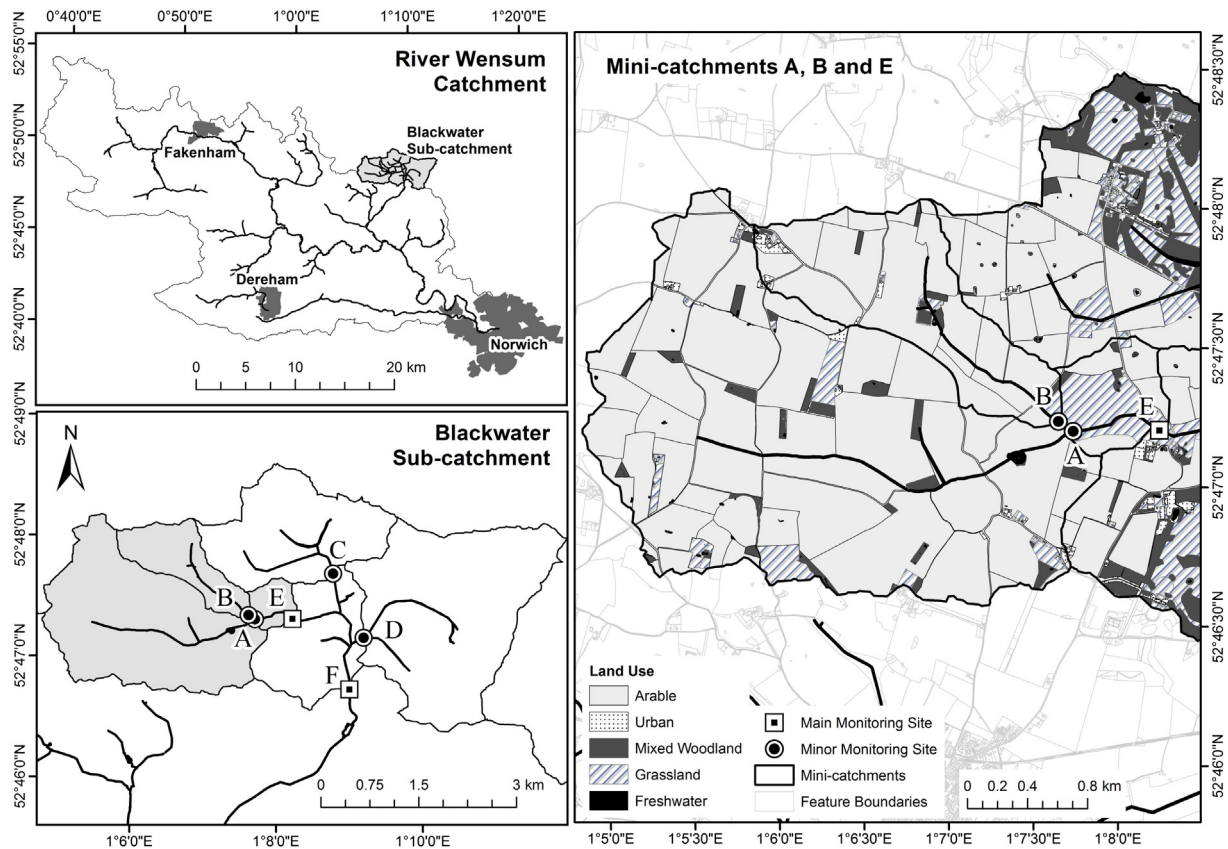
Fig. 1. The Blackwater sub-catchment study area, showing land cover types in mini-catchments A, B and E, with the wider River Wensum catchment also shown.

2.2. Suspended particulate matter sampling

Between May 2012 and March 2014, 6 L stream water grab samples were collected at 1–2 week intervals under baseflow conditions at the outlets to mini-catchments A, B and E, yielding 222 samples in total. During the same period, the bankside automatic water samplers were remotely activated to capture a total of 721 1 L grab samples at 60- or 120-min resolution during 14 storm events at the same locations (where events are characterised by >8 mm of precipitation). All samples were collected at the same depth and location in the centre of the channel to ensure consistency between baseflow and storm event SPM. The stream water samples were returned to the laboratory and vacuum filtered through Millipore quartz fibre filter (QFF) papers with a retention rating of 99.1% at 0.7 μm to extract particulate matter. Sufficient water was filtered to obtain ~25 mg of SPM on each filter. The SPM-covered filters were subsequently oven dried at 105 °C for 2 h and weighed to determine sediment mass retention and instream SPM concentrations.

2.3. Sediment source area sampling

Four sources potentially contributing sediment to the River Blackwater where identified across mini-catchments A and B. These were arable topsoils, damaged road verges, stream channel banks and sub-surface agricultural field drains. Both topsoil and road verge materials were collected as <50 mm surface scrapes from areas susceptible to erosion that had high connectivity with the stream channel (e.g. field entrances, tramlines, narrow road sections). Thirty samples from each of these surface sources were collect in both mini-catchments A and B. Channel bank sediments were sampled as surface scrapes at depths of 10, 30 and 50 cm above the streambed along the full reach of the river as this represented the most heavily eroded section of the banks. Thirty

bank samples were collected from each mini-catchment. Sediments from 148 agricultural field drains identified across the mini-catchments were collected by bulking together grab samples taken over a 12-month period. In total, 30 drain samples were collected from mini-catchment A and 18 from mini-catchment B. In the laboratory, all source area samples were sonicated in a water bath for 7 min and wet sieved to <63 μm to ensure comparable particle sizes and geochemistry with SPM. Approximately 25 mg of these sediments were then vacuum filtered onto QFF papers and oven dried at 105 °C for 2 h. Further details on this sediment source sampling can be found in Cooper et al. (2015).

2.4. Streambed sediment sampling

In support of the SPM sampling, streambed sediments were collected on a single occasion at site E at the end of the study period to investigate evidence of iron sulphide (FeS) formation in the reducing conditions beneath the surface of the streambed. A cylindrical metal soil corer (10 cm diameter × 15 cm depth) was pushed into the centre of the streambed to capture a ~10 cm depth sediment core, of which the upper 6 cm were transferred into an airtight plastic container. To prevent oxidation of any sulphides present within the sample, the sediments were immediately freeze-dried under vacuum for 24 h on return to the laboratory. The dried sediment was sieved to <250 μm to remove large organic debris and stored in airtight polyethylene bags until analysis.

2.5. Spectroscopic analysis

The geochemistry of all SPM-covered filter papers was analysed directly by X-ray fluorescence spectroscopy (XRFS) and diffuse reflectance infrared Fourier transform spectroscopy (DRIFTS) following the procedures described by Cooper et al. (2014). The concentrations of

11 elements (Al, Ca, Ce, Fe, K, Mg, Mn, Na, P, Si, Ti) and five organic and inorganic phases (POC, dithionate-extractable Al (Al_{di}) and Fe (Fe_{di}), oxalate-extractable Al (Al_{ox}) and Fe (Fe_{ox})) were determined. Also calculated were Fe–P ratios, which are a useful indicator of P buffering capacity, and Al/Fe oxalate–dithionate ratios, which effectively quantify the proportion of reactive (amorphous) to less reactive (crystalline) oxyhydroxide phases. The streambed sediments were analysed for FeS by coupled scanning electron microscopy and energy dispersive X-ray spectroscopy (SEM-EDS).

2.6. Statistical analysis

To begin with, the relationships between all measured SPM properties were assessed via correlation panel plots for both baseflow and storm event samples. Then, to obtain a more comprehensive understanding of SPM P control mechanisms, a series of regression analyses were performed for the prediction of P under baseflow and storm event conditions for each of the three sampling locations (A, B and E) such that six analyses were conducted in total. We initially formulated linear mixed effects (LME) models with a temporal random effects component expressed in minutes since the earliest sample using an exponential autoregressive correlation structure and restricted maximum likelihood (REML) to provide unbiased parameter estimates. The purpose of this was to account for autocorrelation in the geochemical time-series data. However, the inclusion of this temporal autocorrelation did not significantly improve the model fit, thus rendering the use of the LME approach redundant. We therefore adopted a simpler multiple linear regression approach based on ordinary least squares (OLS) which was performed in the R environment (R Development Core Team, 2014). Due to heteroscedasticity in the distribution of SPM P values (based on inspection of predictand histograms) these regression analyses were undertaken on log transformed P concentrations. Predictors for all six regression models were selected based on prior knowledge of their associations with P and included:

- (i) Metal oxyhydroxides ($Al_{ox/di}$, $Fe_{ox/di}$) and elements associated with metal oxyhydroxides (Fe, Al, Mn);
- (ii) Elements associated with clay minerals (K, Mg, Na);
- (iii) Calcium (Ca) based on the co-precipitation of P with calcite (House, 2003);
- (iv) Phases associated with organic material (POC);
- (v) Elements strongly associated with particle size (Ti, Si) (Rawlins et al., 2009);
- (vi) Cerium (Ce) based in its enrichment in P-bearing apatite minerals (Rawlins, 2011);
- (vii) Channel stage, because flow volumes influence both SPM transport capacity and its provenance.

A backwards elimination selection procedure was adopted, whereby an initial model including all of the aforementioned predictors was formulated and any statistically insignificant regressors ($p > 0.05$) were then removed one by one until only significant predictors remained. Variance inflation factor (VIF) values were also calculated for each predictor as a measure of multicollinearity. Any predictor with VIF values >10 were considered to have high multicollinearity and were therefore removed from the model to minimise the risk of overfitting the regression. Once this final set of significant predictors had been identified, the relative importance of each regressor was estimated and an independent 10-fold cross-validation procedure was conducted to validate model results.

Lastly, time-series of SPM P concentration, Fe–P ratios and oxalate–dithionate ratios were plotted and inspected for evidence of seasonality during the 23-month monitoring period. We used a 15 point, second order Savitzky–Golay algorithm (Savitzky and Golay, 1964)

to filter the time-series and overlaid these on the plots to aid their interpretation.

3. Results and discussion

3.1. Baseflow geochemistry

Fig. 2 presents the correlation plots for baseflow SPM geochemistry. Immediately apparent are the very strong positive correlations between Al and Mg ($r = 0.95$), Al and K ($r = 0.92$) and Mg and K ($r = 0.84$) which indicate the presence of clay minerals which contain significant amounts of all three cations. Strong positive correlations also exist between Al and Ti ($r = 0.75$), K and Ti ($r = 0.77$) and Na and Mg ($r = 0.72$), further supporting the presence of clay minerals within SPM, with 70% of kaolinite minerals reported to contain Ti (Dolcater et al., 1970). Another notable association is that between Fe and P ($r = 0.71$), which likely indicates P sorbing to the solid phase mineral surfaces of Fe-containing compounds. However, somewhat unexpectedly, P is not correlated with the abundance of either Fe_{di} or Fe_{ox}. This may in part be explained by the occurrence of range of poorly crystalline $Fe^{(II)}$ or mixed $Fe^{(II)}/Fe^{(III)}$ minerals (alongside FeOOH) that have vastly different P binding properties, as observed by Bortleson (1974) based on an analyses of lake sediments. The non-specific nature of oxalate and diothionite extractions likely results in the dissolution of amorphous and crystalline forms of Fe with a wide range of P sorption capacities resulting in a weak overall correlation with total P. There is also no obvious association between P and Ce ($r = 0.19$), in contrast to the findings of Rawlins (2011) who demonstrated that variations in Ce could explain 10.4% of the variability in bed sediment P concentration in rivers across central England.

With respect to the organic fraction, POC exhibits negligible correlation with SPM P ($r = 0.06$) under baseflow conditions, suggesting a dominantly inorganic control on baseflow SPM P concentrations. Instead, POC correlates most strongly with Fe_{ox} ($r = 0.66$), which may be explained by (i) the sorption of POC onto the surfaces of Fe oxyhydroxides which, due to their large specific surface areas, commonly have sorption rates an order of magnitude greater than many common clay minerals; or (ii) the stabilisation and protection from degradation afforded to POC through the formation of organo-Fe complexes (Kaiser and Guggenberger, 2003; Wagai and Mayer, 2007). Furthermore, it has been demonstrated that the amorphous Fe compounds tend to be more important than crystalline oxyhydroxides in this stabilisation process (Wilson et al., 2013). Evidence for this can be seen here, with stronger linear correlations between POC and the amorphous Fe_{ox} ($r = 0.66$) than with crystalline Fe_{di} ($r = 0.15$).

3.2. Storm event geochemistry

Fig. 3 presents the correlation plots for storm event SPM geochemistry. Strong, positive correlations are again apparent between Al and K ($r = 0.93$), Al and Mg ($r = 0.89$) and K and Mg ($r = 0.87$), once more indicating that clay mineral composition likely dominates these geochemical associations. Strong correlations between Al and Ti ($r = 0.82$), K and Ti ($r = 0.84$) and Mg and Ti ($r = 0.79$), indicate Ti oxides in association with these clay minerals. Compared with baseflow conditions, linear correlations between Ce and K ($r = 0.85$), Ce and Al ($r = 0.82$) and Ce and Ti ($r = 0.78$) are substantially stronger, which may reflect an increased supply of SPM from Ce enriched topsoil and road verge sediments during heavy precipitation events (Cooper et al., 2015).

Importantly, P exhibits a strong positive correlation with POC during storm events ($r = 0.56$), in contrast to its association under baseflow conditions. This relationship is consistent with similar findings by Walling et al. (2001) for four other UK rivers (Seven, Avon, Exe and Dart) under storm event flows. POC also correlates strongly with Mn ($r = 0.69$), as does P ($r = 0.51$). Previous research has demonstrated that Mn can be particularly effective in the sorption of P, with freshly
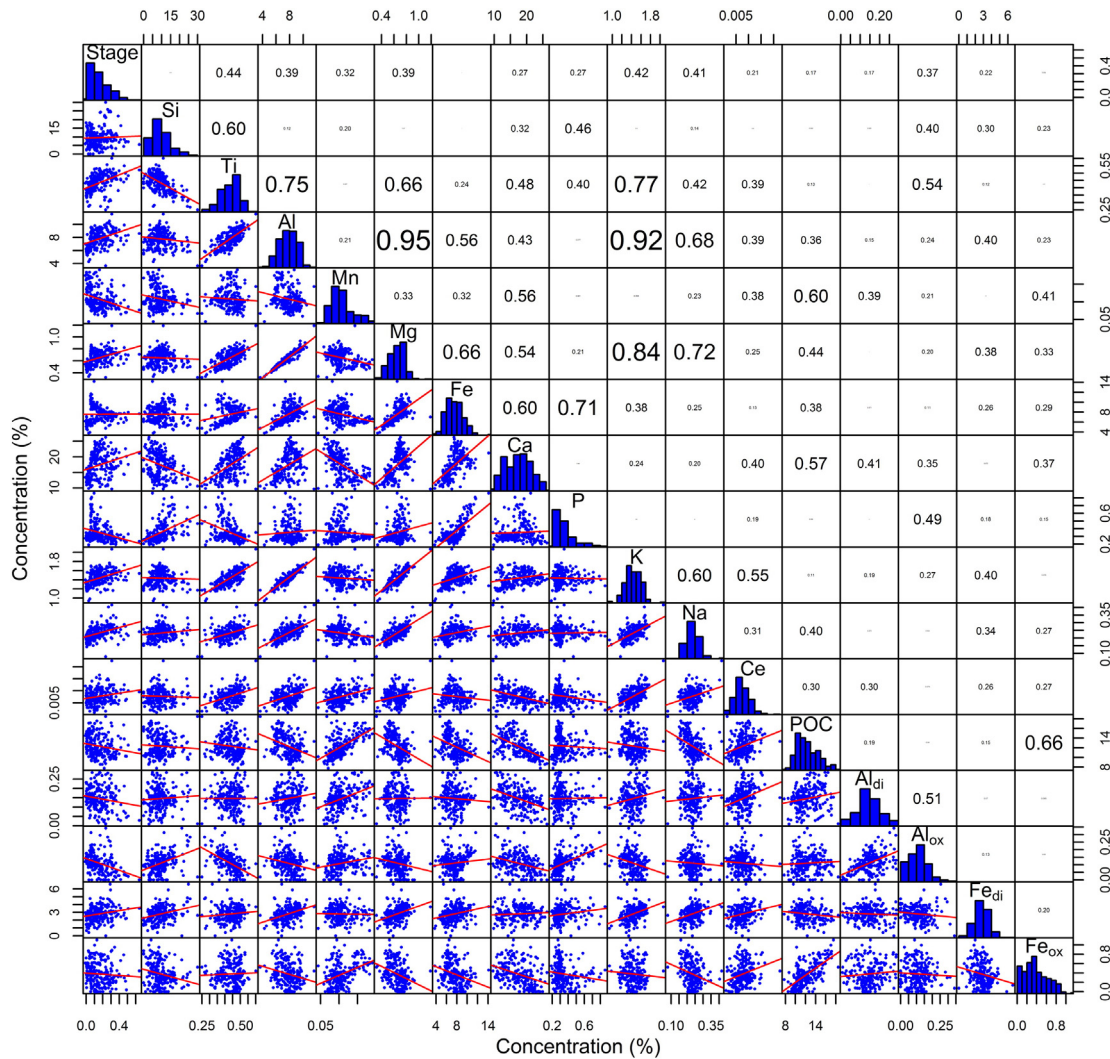
Fig. 2. Correlation panel plot of SPM geochemistry (% by weight) under baseflow conditions at sites A, B and E (*n* = 222). Stage is recorded in metres. The upper right section displays Pearson's correlation coefficients with the text size proportional to correlation strength. The bottom left panel shows the SPM samples (points) and linear regression (line). Central histograms show the distribution of values for each parameter.

precipitated Mn hydroxides (which likely form in streambed sediments under varying redox conditions) found to have a higher P sorption capacities than equivalent Fe or Al hydroxides (Lu and Liao, 1997). However, Lu and Liao (1997) also showed that upon ageing, Mn became the least effective of the three metals in terms of sorption capacity.

3.3. Determining SPM P control mechanisms

3.3.1. Baseflow regression models

The baseflow multiple regression models (Table 2) explain 76–96% of the variance in SPM P concentrations at each of the three sites based on between four and six geochemical predictors. Variation in total Fe concentration is a consistently dominant predictor, explaining 37%, 12% and 38% of SPM P variability at sites A, B and E, respectively. The sorption of P onto the surfaces of Fe containing complexes represents the most likely causal mechanism for this strong, positive Fe–P association. Similarly, sorption of P onto the surfaces of metal oxyhydroxides would explain the significant association with Al_{ox} at site A ($R^2 = 0.156$) and with Mg at site A ($R^2 = 0.049$) and site E ($R^2 = 0.112$). Interestingly, neither K nor Na are significant predictors, suggesting that the quantity or type of clay minerals in SPM is not a dominant control of baseflow SPM P in these catchments.

A strong negative relationship with Ti is observed at site A ($R^2 = 0.224$) and site E ($R^2 = 0.449$), although it is not a significant predictor at site B. The most likely host for Ti is secondary Ti oxides, which tend to be fine-grained and form associations with other mineral phases. If the Ti in SPM is a secondary oxide, its strong linear correlations with Al, K and Mg ($r > 0.66$; Fig. 2) suggest it is closely associated with certain clay minerals which are less enriched in P than Fe containing phases, hence the negative association. At site B, Si is the dominant predictor of SPM P ($R^2 = 0.445$), with this strong, positive association contrasting strongly with the regression results for sites A and E. High SPM Si concentrations typically indicate an abundance of coarse quartz material and thus a strong positive association with P, which tends to be enriched in fine sediment, would not intuitively be expected. However, Si is strongly and negatively associated with Ti ($r = -0.60$; Fig. 2) and thus the association between P and Si at site B may reflect collinearity between these two predictors.

POC is a relatively weak predictor under baseflow conditions, explaining just 1% of the variance in SPM P concentrations at site A and 8% at sites B and E. Similarly, Ce was a weak predictor at site B ($R^2 = 0.062$), whilst Ca was insignificant at all sites implying that abiotically mediated co-precipitation of P with calcite is not an important control of SPM P concentrations. Overall, these multiple regression model results indicate that the abiotic sorption of P onto the surfaces
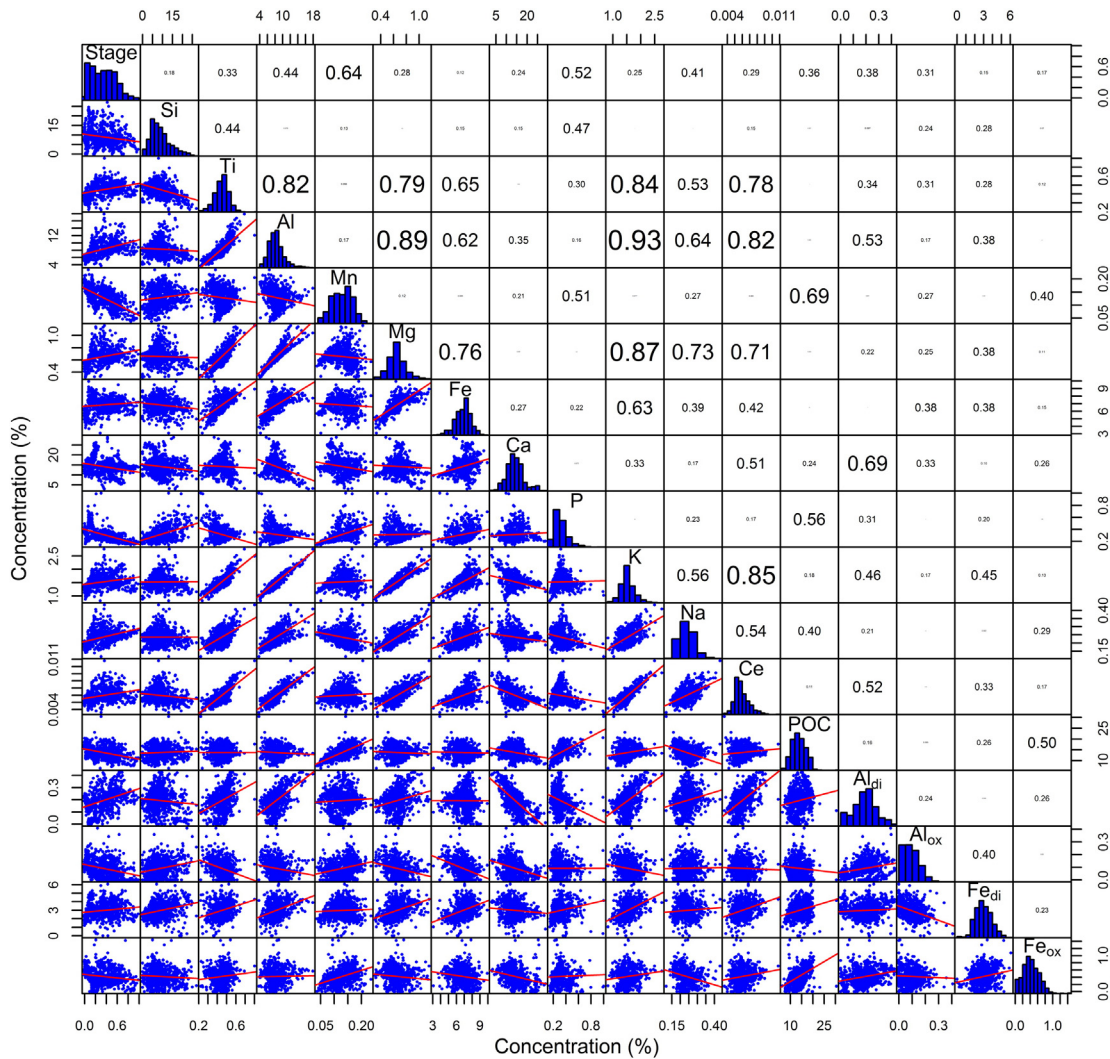
Fig. 3. Correlation panel plot of SPM geochemistry (% by weight) under storm event conditions at sites A, B and E ($n = 721$). Stage is recorded in metres. The upper right section displays Pearson's correlation coefficients with the text size proportional to correlation strength. The bottom left panel shows the SPM samples (points) and linear regression (line). Central histograms show the distribution of values for each parameter.

of Fe containing complexes is a dominant control of baseflow SPM P concentrations in the River Blackwater.

3.3.2. Storm event regression models

The storm event regression models explain 71–94% of the variance in SPM P concentrations across the three sites based on between four and eight predictors (Table 3). Importantly, the results reveal a clear

shift in P association, from Fe-dominated under baseflow conditions to POC-dominated during storm events. Variability in POC concentrations are able explain 21%, 62% and 20% of the variance in SPM P at sites A, B and E, respectively, making it the strongest predictor at two of these locations. This P–POC association may relate to OM being a source of P through mineralization reactions and soluble reactive phosphorus (SRP) sorbing onto the surfaces of OM in soils and sediments. However,

Table 1

Selected geochemistry data for SPM and source area sediments collected in mini-catchments A, B and E of the River Blackwater. μ is the mean, σ is the standard deviation.

SPM/source area	Statistic	Concentrations (weight %)								Fe:P ratio	Fe:POC ratio	Al$_{ox}$:Al$_{di}$ ratio	Fe$_{ox}$:Fe$_{di}$ ratio
		Al	Ca	Ce[a]	Fe	Mg	Mn	P	POC				
Baseflow SPM	μ	7.77	17.34	55	7.56	0.65	0.11	0.35	12.35	22.91	0.64	0.79	0.16
($n = 222$)	σ	1.31	3.91	6	1.62	0.12	0.03	0.13	2.13	5.58	0.20	0.41	0.15
Storm event SPM	μ	8.29	14.24	60	6.87	0.66	0.13	0.32	13.78	23.44	0.52	0.62	0.15
($n = 721$)	σ	1.99	4.16	9	0.98	0.13	0.04	0.11	2.97	6.57	0.13	0.69	0.09
Channel banks	μ	6.63	33.92	37	4.74	0.63	0.02	0.07	2.21	76.33	3.22	0.18	0.43
($n = 60$)	σ	2.35	9.80	16	1.78	0.19	0.03	0.03	2.01	27.20	1.84	0.25	0.61
Field drains	μ	6.66	14.25	60	6.88	0.53	0.19	0.27	7.89	33.67	0.98	1.00	0.42
($n = 48$)	σ	2.96	10.75	28	4.59	0.27	0.26	0.26	3.61	15.04	0.66	0.67	0.78
Road verges	μ	10.50	4.82	88	5.55	0.91	0.16	0.32	12.96	17.59	0.45	0.44	0.26
($n = 60$)	σ	1.76	2.13	8	0.90	0.20	0.03	0.04	2.39	3.87	0.12	0.19	0.14
Topsoils	μ	14.23	3.18	94	6.53	0.84	0.12	0.29	10.22	23.90	0.67	0.63	0.25
($n = 60$)	σ	1.91	3.29	11	0.83	0.11	0.02	0.07	2.30	6.71	0.17	0.14	0.16

[a] Ce concentration in ppm.

Table 2
Baseflow multiple linear regression model results for the prediction of log-P at sites A (n = 74), B (n = 74) and E (n = 74) between May 2012 and March 2014. VIF is the variance inflation factor; VE is the variance explained; CV is the independent 10-fold cross-validation.

Predictor	Estimate	Std. error	t-Value	p-Value	VIF	Proportion of VE (R^2)
Site A						
Fe	0.147	0.010	15.29	<0.001	1.03	0.370
Ti	−3.865	0.418	−9.24	<0.001	3.47	0.224
Al$_{ox}$	1.357	0.310	4.37	<0.001	2.34	0.156
POC	0.058	0.009	6.16	<0.001	1.15	0.078
Mg	1.160	0.196	5.92	<0.001	2.47	0.048
Al$_{di}$	−1.062	0.275	−3.86	<0.001	1.50	0.020
					Total R^2	0.895
					CV R^2	0.850
Site B						
Si	0.023	0.002	12.84	<0.001	1.45	0.445
Fe	0.115	0.018	6.34	<0.001	3.64	0.123
POC	0.017	0.005	3.36	<0.001	1.95	0.078
Ce	−92.764	16.291	−5.69	<0.001	2.20	0.062
Mn	0.955	0.268	3.57	<0.001	1.60	0.049
					Total R^2	0.757
					CV R^2	0.716
Site E						
Ti	−4.090	0.219	−18.69	<0.001	3.76	0.449
Fe	0.131	0.008	17.39	<0.001	1.70	0.382
Mg	0.880	0.181	4.86	<0.001	5.43	0.112
POC	0.027	0.006	4.47	<0.001	1.62	0.014
					Total R^2	0.957
					CV R^2	0.950

Table 3
Storm event multiple linear regression model results for the prediction of log-P in SPM at sites A (n = 254), B (n = 251) and E (n = 216) between May 2012 and March 2014. VIF is the variance inflation factor; VE is the variance explained; CV is the independent 10-fold cross-validation.

Predictor	Estimate	Std. error	t-Value	p-Value	VIF	Proportion of VE (R^2)
Site A						
Mn	2.184	0.259	8.43	<0.001	3.73	0.275
POC	0.042	0.003	13.65	<0.001	2.56	0.212
Stage	−0.281	0.035	−8.01	<0.001	2.65	0.182
Fe	0.117	0.010	11.55	<0.001	3.25	0.101
K	0.557	0.062	8.95	<0.001	7.59	0.078
Ti	−2.360	0.201	−11.76	<0.001	6.99	0.043
Al$_{di}$	−0.844	0.094	−8.96	<0.001	2.01	0.031
Fe$_{di}$	−0.046	0.007	−6.74	<0.001	1.38	0.013
					Total R^2	0.936
					CV R^2	0.927
Site B						
POC	0.074	0.003	24.53	<0.001	1.44	0.619
Si	0.014	0.001	8.35	<0.001	1.19	0.038
Fe$_{di}$	−0.076	0.009	−8.49	<0.001	1.99	0.037
Al	0.021	0.003	6.62	<0.001	1.79	0.019
					Total R^2	0.714
					CV R^2	0.701
Site E						
POC	0.052	0.003	17.48	<0.001	1.68	0.200
Si	0.019	0.002	9.84	<0.001	4.06	0.174
Mn	1.527	0.255	6.00	<0.001	1.88	0.165
Ti	−2.123	0.251	−8.45	<0.001	9.84	0.150
Al$_{di}$	−0.957	0.078	−12.30	<0.001	1.44	0.130
Fe	0.136	0.010	13.35	<0.001	1.91	0.055
Mg	0.619	0.135	4.60	<0.001	5.39	0.035
Fe$_{di}$	−0.055	0.009	−6.13	<0.001	1.68	0.031
					Total R^2	0.940
					CV R^2	0.932

organic molecules also liberate phosphate ions into solution by replacing them on clay mineral and metal oxyhydroxide surface binding sites, whilst also blocking the pore spaces of mineral aggregates and acting as a protective barrier around mineral surfaces (Kaiser and Guggenberger, 2003; Wagai et al., 2013). Despite these opposing processes, numerous studies have commented upon the link between P and OM in stream sediments, with most establishing similar positive associations to that observed here (e.g. Rawlins, 2011; Krueger et al., 2012).

In further contrast to the baseflow regression models, Mn is a strong and significant predictor of P during storm events at site A ($R^2 = 0.275$) and site E ($R^2 = 0.165$). This likely reflects both Mn association with POC ($r = 0.69$; Fig. 3) and the sorption of P onto the surfaces of metal oxides. Channel stage is also a strong and significant predictor at site A ($R^2 = 0.182$), indicating a dilution of SPM P concentrations under larger flows. Despite its much reduced importance, Fe remains a significant predictor of P during storm events at site A ($R^2 = 0.101$) and site E ($R^2 = 0.055$), confirming the sorption of P onto Fe containing complexes. Significant associations are again evident with Ti at sites A ($R^2 = 0.043$) and E ($R^2 = 0.150$), and with Si at sites B ($R^2 = 0.038$) and E ($R^2 = 0.174$), but these regressors are generally weaker predictors than that observed in the baseflow models. Overall, these multiple regression models indicate that storm event SPM P concentrations are dominantly associated with organic matter complexes.

3.3.3. Interpreting regression results

The pronounced transition from Fe–P dominated associations under baseflow conditions to POC–P associations during storm events can most likely be explained by a change in SPM source area. Previous sediment fingerprinting research in the same catchment (Cooper et al., 2015) demonstrated baseflow SPM source contributions are dominated by subsurface inputs (i.e. stream channel banks and agricultural field drains) which have significantly (t-test $p < 0.01$) larger Fe–POC ratios compared with surface sources (i.e. road verge material and arable topsoils) (Table 1). This creates geochemical conditions conducive to the sorption of phosphate ions onto the surfaces of Fe containing complexes, hence the dominance of the Fe-P association during baseflow. This association may arise in either the stream, soil or field drains as a consequence of changing redox conditions initiating the precipitation of Fe bound P (Jarvie et al., 2008). Conversely, during storm events, SPM was demonstrated to comprise a greater contribution from surface sources which have significantly (t-test $p < 0.01$) smaller Fe–POC ratios (Table 1). This results in larger quantities of P being either transported with, or sorbed onto the surfaces of, OM-bearing complexes, hence the greater importance of the P–POC association observed in the storm event regression models.

The data also indicate that another distinct source of Fe-enriched SPM is mobilised during storm events. Evidence for this comes from examining the SPM Fe-P ratios which increase during large storm events relative to baseflow conditions (Fig. 4). Because surface soils have substantially lower Fe–P ratios than subsurface sediments (Table 1), we hypothesise this increase in the Fe–P ratio of SPM is caused by storm event mobilisation of iron sulphide (FeS) which commonly forms in the reducing conditions beneath the surface of streambeds (Large et al., 2001). Results from the SEM-EDS analysis of sediments collected from the surface of the streambed (0–6 cm depth) at site E confirm the presence of FeS within the easily mobilised fine (<63 μm) sediment fraction, thus supporting this hypothesis (Fig. 5).

3.4. Temporal trends in baseflow SPM composition

3.4.1. Phosphorus

Fig. 6 presents the time-series of SPM P concentrations under baseflow conditions at 1–2 week intervals between May 2012 and March 2014. Whilst no consistent temporal trend is recorded across the three sites, a very strong seasonal cycle is recorded at site E with
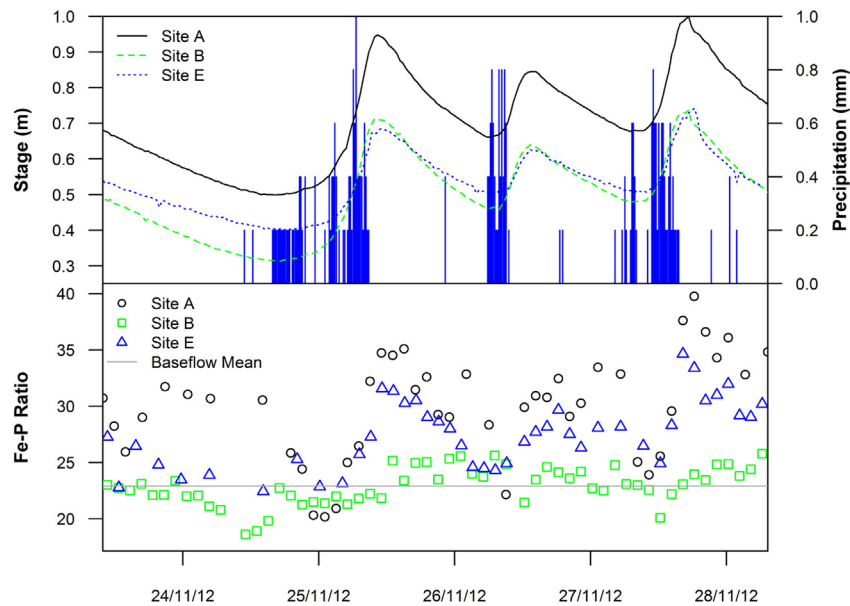
Fig. 4. Time-series of SPM Fe–P ratios for sites A, B and E during three consecutive storm events in November 2012. Baseflow mean refers to the average for all three sites.

larger concentrations during the summer/autumn and smaller during the winter/spring. The timing of these peaks may be linked to a combination of (i) increased autochthonous P release as a consequence of growing season primary production; (ii) the development of P-rich biofilms around fine particulates which grow more vigorously during the summer; (iii) enhanced bed sediment P sorption under low flows; or (iv) increased P-rich SPM inputs from subsurface field drains. These summer/autumn P peaks correspond with similar findings for a range of other UK rivers under differing hydrological conditions (Walling et al., 2001; Stutter et al., 2008; Ballantine et al., 2009).
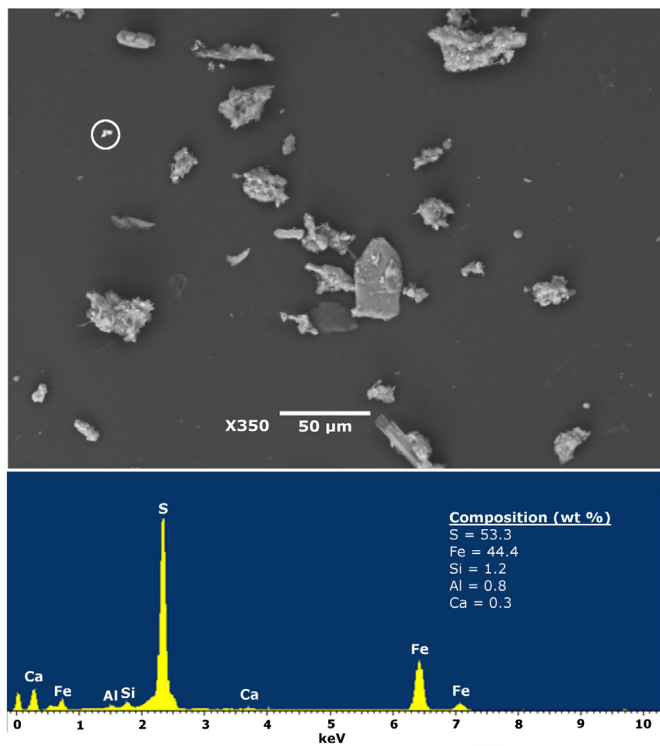

Fig. 5. Evidence of iron sulphides revealed by an SEM-EDS analysis of sediment collected from the streambed surface (0–6 cm depth) at site E. White circle indicates the analysed grain.
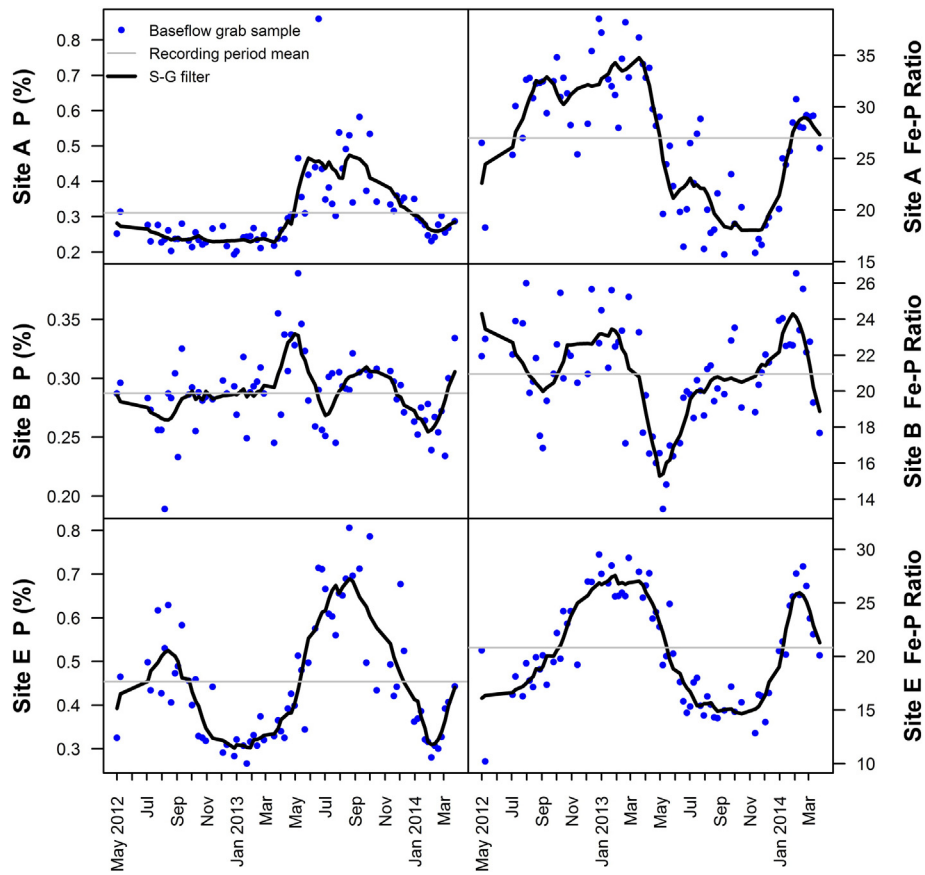
Conversely, SPM P concentrations at site B exhibited three local minima in August 2012, July 2013 and January 2014 and a global maximum in April 2013, whilst concentrations at site A were small and stable between May 2012 and April 2013 before rising sharply during summer 2013. Previous studies have linked such spatial intra-catchment variability in P concentrations to differences in geology, land-use and point sources of pollution such as sewage treatment works (e.g. Ballantine et al., 2008). However, considering the short distance between sites A, B E (600 m) and the absence of any sewage discharges between them, we can rule these out as explanatory factors. Instead, these spatial differences in SPM P concentration likely relate to localised instream primary production and inputs from agricultural field drains which have previously been shown to be important pathways for SPM in this catchment (Cooper et al., 2015) and may transport SRP from agricultural fertilizers directly into the stream channel. It is also worth noting that summer 2013 was warmer (mean monthly temperature 0.5 °C higher) and drier (mean monthly precipitation 45 mm lower) than summer 2012, conditions conducive to vigorous instream primary productivity which may partly explain the higher P peaks observed at all sites during 2013.

3.4.2. Iron–phosphorous ratios

Previous research has demonstrated that Fe–P ratios can be useful indicators of the P buffering capacity of aquatic sediments (Jensen et al., 1992). Specifically, the higher the Fe–P ratio, the greater the potential for the adsorption of SRP onto the surfaces of Fe containing compounds within sediments. Thus, higher Fe–P ratios allow sediment to isolate SRP from uptake by biota and thereby minimise the risk of eutrophication.

In the River Blackwater, baseflow SPM Fe–P ratios during winter/spring 2012 were approximately double that recorded during the following summer/autumn, particularly at sites A and E (Fig. 6). This implies SPM had greater capacity to adsorb excess SRP outside of the growing season. Strong, negative linear correlations between the Fe–P ratio and SPM P at sites A ($r = -0.78$), B ($r = -0.56$) and E ($r = -0.84$) indicate variation in SPM P concentration, and not SPM Fe, was the main driver behind variability in these ratios. This could be explained by greater autochthonous P production during the summer leading to greater P sorption onto Fe-bearing sediments which lowered the Fe–P ratios during the summer months. For all sites, Fe–P ratios observed across the seasons were within the range of values (1–290) reported by House and Denison (2002) for six British rivers and

Fig. 6. Time-series of P concentration and Fe–P ratios in SPM at sites A, B and E under baseflow conditions between May 2012 and March 2014. The smooth lines are 15 point, second order Savitzky–Golay filters.

generally greater than 15, the value above which it has been shown sediments can moderate temporal SRP variability in lacustrine environments (Jensen et al., 1992).

3.4.3. Oxalate–dithionate ratios

The ratio of oxalate-extractable (amorphous) to dithionate-extractable (crystalline) Fe and Al can be used as an index of the P sorption capacity of SPM. The time-series presented in Fig. 7 reveal a clear seasonal cycle in the Al_{ox}–Al_{di} ratios at all sites, with a greater proportion of reactive amorphous material present during the summer months and less during the winter. This cycle is primarily driven by variation in the amorphous Al_{ox} fraction, which correlates strongly and positively with the Al_{ox}–Al_{di} ratios at sites A ($r = 0.78$), B ($r = 0.53$) and E ($r = 0.57$). In contrast with the Fe–P ratios, these Al_{ox}–Al_{di} ratios imply that SPM during the biologically sensitive summer season had a higher P adsorption capacity and thus greater ability to capture and transport SRP through the stream network. This conclusion is supported by the correlation between P and Al_{ox} under baseflow conditions ($r = 0.49$), which was the strongest association of the four Fe and Al oxyhydroxide compounds, and second only to total Fe ($r = 0.71$) for overall correlation with SPM P (Fig. 2).

Based on the composition of sediment source areas (Table 1), we can hypothesise that field drains with enriched Al_{ox}–Al_{di} ratios supplied a greater proportion of Al_{ox} during the summer, whilst contributions from channel banks and road verges with lower Al_{ox}–Al_{di} ratios were more significant during the winter. Therefore, the SPM discharged by agricultural field drains appears to play an important role in determining the transport of SPM P during the growing season when streams are more sensitive to the detrimental effects of eutrophication. However, other processes may also be contributing to the higher proportion of Al_{ox} observed during the summer months. For example, Violante and

Violante (1980) demonstrated that higher concentrations of organic ligands slow down the crystallisation of Al oxyhydroxides (i.e. the formation of Al_{di}). During the growing season, plants release larger quantities of organic acids into soil solution which would restrict the formation of Al_{di} and thus increase the proportion of Al_{ox}, thereby accounting for the higher Al_{ox}–Al_{di} ratios observed in SPM during this period.

Interestingly, both the magnitude and timing of maxima and minima in Al_{ox}–Al_{di} ratios are different between years, with the winter 2012/13 minima occurring ~2 months earlier and being considerably more pronounced than during the corresponding winter 2013/14, for example. This can be explained by a combination of higher rainfall totals and different crop cultivation practices during autumn 2012 altering the sources of SPM compared with the following year.

Seasonality in the Fe_{ox}–Fe_{di} ratios is much less apparent than that observed for Al_{ox}–Al_{di} (Fig. 7) and based on the overall weakness of these trends we cannot make any conclusive statements regarding seasonality in these ratios.

3.5. Significance and further research

Through our analysis of large numbers of SPM samples collected under small and large flows at three adjacent agricultural catchment locations, we present clear evidence of a pronounced change in SPM P control mechanisms; from Fe-dominated associations under baseflow conditions, to POC-dominated associations during storm events. Because the most likely cause of this change is a shift in SPM source area under different hydrological conditions, this is likely to be a widespread phenomenon. This finding has implications for mitigation measures aimed at reducing fluvial SPM P transfers in agricultural catchments, suggesting that different sediment source areas need to be targeted to reduce P contributions under differing hydrological conditions. This
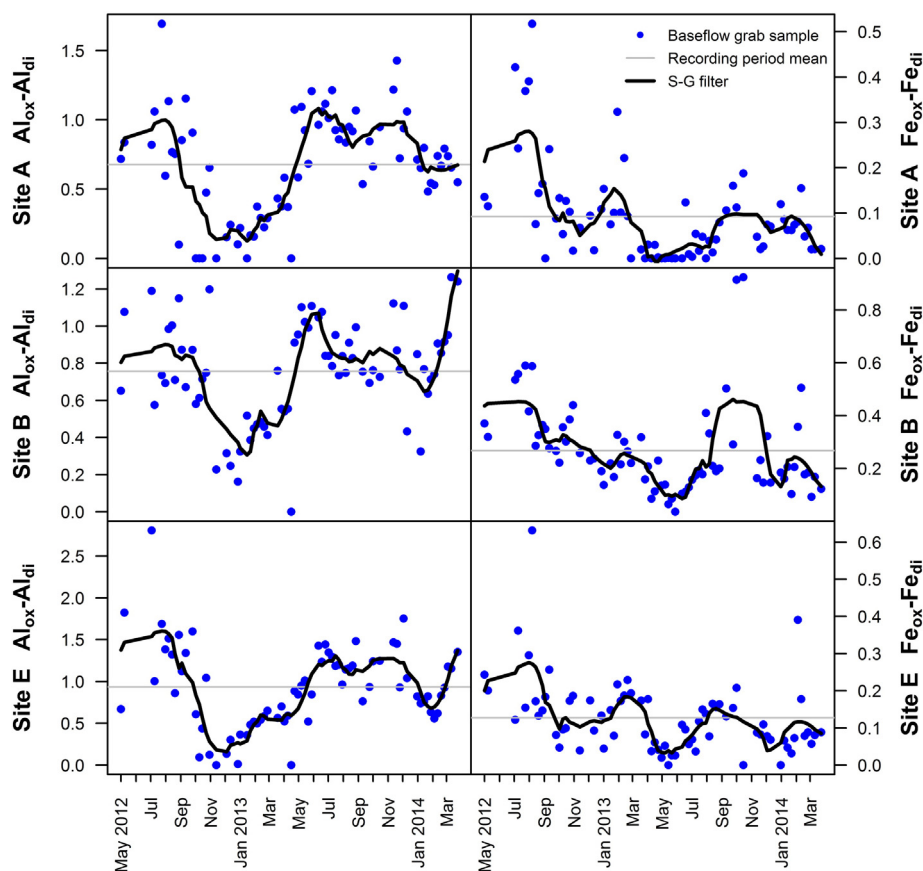
Fig. 7. Ratios of oxalate vs. dithionate extractable Al and Fe in baseflow SPM at sites A, B and E between May 2012 and March 2014. The smooth black line is a 15 point, second order Savitzky–Golay filter.

could include the installation of roadside sediment traps to capture P-rich particulates in surface runoff during storm events (Cooper et al., 2015), or the employment of minimum cultivation techniques to minimise preferential flows of nutrients through subsurface drainage networks under baseflow conditions (Stevens and Quinton, 2009).

Furthermore, to our knowledge, this is the first study to demonstrate distinct seasonality in SPM Al_{ox}–Al_{di} ratios in an agricultural headwater catchment. This observation has important implications for (i) understanding the extent of P availability for exchange between dissolved and particulate forms and (ii) for the development of eutrophic conditions during the ecologically sensitive summer period. The European wide study by Hartikainen et al. (2010) showed that both equilibrium P concentration (the 'zero point' of P exchange at which no net desorption from, or sorption to, sediment occurs) and the quantity of instantly labile P were strongly correlated with the P saturation degree of Al oxyhydroxides. The larger surface area and associated exchange capacity of amorphous, compared to crystalline, Al oxyhydroxides will likely alter their degree of P saturation (Bohn et al., 1979). The degree of P saturation of Al oxyhydroxides may differ between summer and winter due to the differences in the proportions of amorphous and crystalline phases we observed in each of the three streams we studied, so comparisons between P saturation of Al oxyhydroxides in suspended and bed sediments of other headwater channels during winter and summer warrants further investigation.

Lastly, the enriched Al_{ox}–Al_{di} ratios of SPM derived from agricultural field drains indicates that these subsurface drainage networks, which are widespread throughout the intensive arable systems of Europe and North America, are potentially important for controlling the instream concentration of reactive P. Consequently, mitigation measures aimed at reducing SPM discharges from field drains could

decrease the amount of Al_{ox} associated P in agricultural headwater streams.

4. Conclusions

In this study, we have used large numbers of SPM samples collected under baseflow ($n = 222$) and storm event ($n = 721$) conditions to demonstrate contrasting control mechanisms on SPM P concentration under different flow regimes in three lowland agricultural headwater catchments. Multiple linear regression models reveal a pronounced shift in P association, from Fe-dominated under baseflow conditions to POC-dominated during storm events. It is hypothesised that this transition in P control mechanism, which is spatially consistent across the three study catchments, is driven by changes in the dominant SPM source area. Specifically, greater SPM supply is thought to originate from subsurface stream channel banks and agricultural field drains with comparatively high Fe–POC ratios during baseflow conditions, coupled with increased autochthonous P contributions. Conversely, contributions from surface soils with comparatively depleted Fe–POC ratios are thought to increase during storm events, along with the erosive mobilisation of iron sulphide from beneath the surface of the streambed. Further examination of weekly baseflow data revealed evidence of seasonality in both Fe–P and Al oxalate–dithionate (Al_{ox}–Al_{di}) ratios over a 23-month period. This indicates temporal variability in the P sorption capacity of SPM and is thought to relate to both changes in SPM source area and the quantity of organic ligands which inhibit the crystallisation of Al oxyhydroxides. The results presented here significantly enhance our understanding of the contrasting control mechanisms of SPM P under varying flow regimes and have

important implications for the targeting of P mitigation measures in agricultural catchments under different hydrological conditions.

Supplementary data to this article can be found online at http://dx.doi.org/10.1016/j.scitotenv.2015.06.113.

References

Ballantine, D.J., Walling, D.E., Collins, A.L., Leeks, G.J.L., 2008. The phosphorus content of fluvial suspended sediment in three lowland groundwater-dominated catchments. J. Hydrol. 357, 140–151. http://dx.doi.org/10.1016/j.jhydrol.2008.05.011.
Ballantine, D.J., Walling, D.E., Collins, A.L., Leeks, G.J.L., 2009. The content and storage of phosphorus in fine-grained channel bed sediment in contrasting lowland agricultural catchments in the UK. Geoderma 151, 141–149. http://dx.doi.org/10.1016/j.geoderma.2009.03.021.
Bohn, H.L., McNeal, B.L., O'Connor, G.A., 1979. Soil chemistry. John Wiley & Sons, New York.
Bortleson, G.C., 1974. Phosphorus, iron and manganese distribution in sediment cores of six Winconsin lakes. Limnol. Oceanogr. 19, 794–801.
Bowes, M.J., House, W.A., Hodgkinson, R.A., 2003. Phosphorus dynamics along a river continuum. Sci. Total Environ. 313, 119–212. http://dx.doi.org/10.1016/S0048-9697(03)00260-2.
Cooper, R.J., Rawlins, B.G., Lézé, B., Krueger, T., Hiscock, K., 2014. Combining two filter paper-based analytical methods to monitor temporal variations in the geochemical properties of fluvial suspended particulate matter. Hydrol. Process. 28, 4042–4056. http://dx.doi.org/10.1002/hyp.9945.
Cooper, R.J., Krueger, T., Hiscock, K.M., Rawlins, B.G., 2015. High-temporal resolution fluvial sediment source fingerprinting with uncertainty: a Bayesian approach. Earth Surf. Process. Landf. 40, 78–92. http://dx.doi.org/10.1002/esp.3621.
Dolcater, D.L., Syers, J.K., Jackson, M.L., 1970. Titanium as free oxide and substituted forms in kaolinites and other soil minerals. Clay Clay Miner. 18, 71–79.
Evans, D.J., Johnes, P.J., Lawrence, D.S., 2004. Physico-chemical controls on phosphorus cycling in two lowland streams. Part 2 — the sediment phase. Sci. Total Environ. 329, 165–182. http://dx.doi.org/10.1016/j.scitotenv.2004.02.023.
Hartikainen, H., Rasa, K., Withers, P.J.A., 2010. Phosphorus exchange properties of European soils and sediments derived from them. Eur. J. Soil Sci. 6, 1033–1042. http://dx.doi.org/10.1111/j.1365-2389.2010.01295.x.
Hilton, J., O'Hare, M., Bowes, M.J., Jones, J.I., 2006. How green is my river? A new paradigm of eutrophication in rivers. Sci. Total Environ. 365, 66–83. http://dx.doi.org/10.1016/j.scitotenv.2006.02.055.
Hiscock, K.M., Dennis, P.F., Saynor, P.R., Thomas, M.O., 1996. Hydrochemical and stable isotope evidence for the extent and nature of the effective Chalk aquifer of north Norfolk, UK. J. Hydrol. 180, 79–107. http://dx.doi.org/10.1016/0022-1694(95)02895-1.
House, W.A., 2003. Geochemical cycling of phosphorus in rivers. Appl. Geochem. 18, 739–748. http://dx.doi.org/10.1016/S0883-2927(02)00158-0.
House, W.A., Denison, F.H., 2002. Total phosphorus content of river sediments in relationship to calcium, iron and organic matter concentrations. Sci. Total Environ. 282–283, 341–351. http://dx.doi.org/10.1016/S0048-9697(01)00923-8.
House, W.A., Warwick, M.S., 1999. Interactions of phosphorus with sediments in the River Swale, Yorkshire, UK. Hydrol. Process. 13, 1103–1115.
Jarvie, H.P., Haygarth, P.M., Neal, C., Butler, P., Smith, B., Naden, P.S., Joynes, A., Neal, M., Wickham, H., Armstrong, L., Harman, S., Palmer-Felgate, E.J., 2008. Stream water chemistry and quality along an upland–lowland rural land-use continuum, south west England. J. Hydrol. 350, 215–231. http://dx.doi.org/10.1016/j.jhydrol.2007.10.040.

Jensen, H.S., Kristensen, P., Jeppesen, E., Skytthe, A., 1992. Iron:phosphorus ratio in surface sediments as an indicator of phosphate release from aerobic sediments in shallow lakes. Hydrobiologia 235–236, 731–743.
Kaiser, K., Guggenberger, G., 2003. Mineral surfaces and soil organic matter. Eur. J. Soil Sci. 54, 219–236. http://dx.doi.org/10.1046/j.1365-2389.2003.00544.x.
Krueger, T., Quinton, J.N., Freer, J., Macleod, C.J.A., Bilotta, G.S., Brazier, R.E., Hawkins, J.M.B., Haygarth, P.M., 2012. Comparing empirical models for sediment and phosphorus transfer from soils to water at field and catchment scale under data uncertainty. Eur. J. Soil Sci. 63, 211–223. http://dx.doi.org/10.1111/j.1365-2389.2011.01419.x.
Large, D.J., Fortey, N.J., Milodowski, A.E., Christy, A.G., Dodd, J., 2001. Petrographic observations of iron, copper, and zinc sulphides in freshwater canal sediment. J. Sediment. Res. 71, 61–69. http://dx.doi.org/10.1306/052600710061.
Lewis, M.A., 2011. Borehole drilling and sampling in the Wensum demonstration test catchment. British Geological Survey Commissioned Report, CR/11/162. National Environment Research Council, Keyworth, Nottingham, UK (38 pp.).
Lu, Q., Liao, Z., 1997. Comparative study on characteristics of P fixation by Mn, Fe and Al. Pedosphere 7, 325–330.
Outram, F.N., Lloyd, C.E.M., Jonczyk, J., Benskin, C.M.H., Grant, F., Perks, M.T., Deasy, C., Burke, S.P., Collins, A.L., Freer, J., Haygarth, P.M., Hiscock, K.M., Johnes, P.J., Lovett, A.L., 2014. High-frequency monitoring of nitrogen and phosphorus response in three rural catchments to the end of the 2011–2012 drought in England. Hydrol. Earth Syst. Sci. 18, 3429–3448. http://dx.doi.org/10.5194/hess-18-3429-2014.
Palmer-Felgate, E.J., Jarvie, H.P., Withers, P.J.A., Mortimer, R.J.G., Krom, M.D., 2009. Streambed phosphorus in paired catchments with different agricultural land use intensity. Agric. Ecosyst. Environ. 134, 53–66. http://dx.doi.org/10.1016/j.agee.2009.05.014.
Quinton, J.N., Govers, G., Oost, K.V., Bardgett, R.D., 2010. The impact of agricultural soil erosion on biogeochemical cycling. Nat. Geosci. 3, 311–314. http://dx.doi.org/10.1038/NGEO838.
R Development Core Team, 2014. R: a language and environment for statistical computing. R Foundation for Statistical Computing, Vienna, Austria (http://www.R-project.org).
Rawlins, B.G., 2011. Controls on the phosphorus content of fine stream bed sediment in agricultural headwater catchments at the landscape scale. Agric. Ecosyst. Environ. 144, 352–363. http://dx.doi.org/10.1016/j.agee.2011.10.002.
Rawlins, B.G., Webster, R., Tye, A.M., Lawley, R., O'Hara, S.L., 2009. Estimating particle-size fractions of soil dominated by silicate minerals from geochemistry. Eur. J. Soil Sci. 60, 116–126. http://dx.doi.org/10.1111/j.1365-2389.2008.01112.x.
Savitzky, A., Golay, M.J., 1964. Smoothing and differentiation of data by simplified least square procedures. Anal. Chem. 36, 1627–1639. http://dx.doi.org/10.1021/ac60214a047.
Smith, V.H., Tilman, G.D., Nekola, J.C., 1999. Eutrophication: impacts of excess nutrient inputs on freshwater, marine, and terrestrial ecosystems. Environ. Pollut. 100, 179–196. http://dx.doi.org/10.1016/S0269-7491(99)00091-3.
Stevens, C., Quinton, J., 2009. Diffuse pollution swapping in arable agricultural systems. Crit. Rev. Environ. Sci. Technol. 39, 478–520. http://dx.doi.org/10.1080/10643380801910017.
Stutter, M.I., Langan, S.J., Cooper, R.J., 2008. Spatial and temporal dynamics of stream water particulate and dissolved N, P and C forms along a catchment transect, NE Scotland. J. Hydrol. 350, 187–202. http://dx.doi.org/10.1016/j.jhydrol.2008.08.002.
Van der Perk, M., Owens, P.N., Deeks, L.K., Rawlins, B.G., Haygarth, P.M., Beven, K.J., 2007. Controls on catchment-scale patterns of phosphorus in soil, streambed sediment, and stream water. J. Environ. Qual. 36, 694–708. http://dx.doi.org/10.2134/jeq2006.0175.
Violante, A., Violante, P., 1980. Influence of pH, concentration, and chelating power of organic anions on the synthesis of aluminium hydroxides and oxyhydroxides. Clay Clay Miner. 28, 425–434.
Wagai, R., Mayer, L.M., 2007. Sorptive stabilization of organic matter in soils by hydrous iron oxides. Geochim. Cosmochim. Acta 71 (25), 35. http://dx.doi.org/10.1016/j.gca.2006.08.047.
Wagai, R., Mayer, L.M., Kitayama, K., Shirato, Y., 2013. Association of organic matter with iron and aluminium across a range of soils determined via selective dissolution techniques coupled with dissolved nitrogen analysis. Biogeochemistry 112, 95–109. http://dx.doi.org/10.1007/s10533-011-9652-5.
Walker, T.W., Syers, J.K., 1976. The fate of phosphorus during pedogenesis. Geoderma 15, 1–19. http://dx.doi.org/10.1016/0016-7061(76)90066-5.
Walling, D.E., Webb, B.W., Russell, M.A., 1997. Sediment-associated nutrient transport in UK rivers. In: Webb, B. (Ed.), Freshwater Contamination. IAHS Publication, pp. 69–81.
Walling, D.E., Russell, M.A., Webb, B.W., 2001. Controls on the nutrient content of suspended sediment transported by British rivers. Sci. Total Environ. 266, 113–123. http://dx.doi.org/10.1016/S0048-9697(00)00746-4.
Wilson, C.A., Cloy, J.M., Graham, M.C., Hamlet, L.E., 2013. A microanalytical study of iron, aluminium and organic matter relationships in soils with contrasting hydrological regimes. Geoderma 202–203, 71–81. http://dx.doi.org/10.1016/j.geoderma.2013.03.020.
Withers, P.J.A., Jarvie, H.P., 2008. Delivery and cycling of phosphorus in rivers: a review. Sci. Total Environ. 400, 379–395. http://dx.doi.org/10.1016/j.scitotenv.2008.08.002.